Parabola Volume 57, Issue 1 (2021)

A meteorological application of the Euler spiral map projection

Timothy Hume[1]

1 Introduction

The Euler spiral map projection is an unusual map projection that results from flattening a spherical spiral onto a flat surface. It was popularised in a video featuring mathematician Hannah Fry [4] and is based on the maths in a short 2012 paper by Bartholdi and Henriques [1]. Figure 1 shows an example of the Euler spiral map projection.

Figure 1: Example of the Euler spiral map projection. Image generated from the website `http://andersk.mit.edu/euler-spiral-projection/`.

At first sight, the Euler spiral map projection does not appear very practical. For example, the spiral dissects many countries on the map. However, concepts that initially appear to have limited practical use are often later found to have unexpected applications. This article shows how the Euler spiral map projection can be used to compress meteorological data. Additionally, it has several other interesting properties which make it useful for meteorology.

However, first we present a brief introduction to numerical weather prediction and cartography for readers unfamiliar with these subjects.

[1]Tim Hume (tim@nomuka.com) works as a meteorologist.

Numerical weather prediction

Numerical weather prediction (NWP) has had a significant impact on weather forecasting. It has enabled the production of weather forecasts for up to a week or more into the future. NWP solves the equations of atmospheric motion using numerical techniques. Richardson pioneered NWP in his 1922 book *Weather Prediction by Numerical Process* [7]. However, at the time computations were only able to be performed manually, making the method impractical. The first modern NWP forecast was produced in 1950, using the ENIAC computer (Figure 2). A forecast for the North American region twenty-four hours into the future took about twenty-four hours of computer time [3].

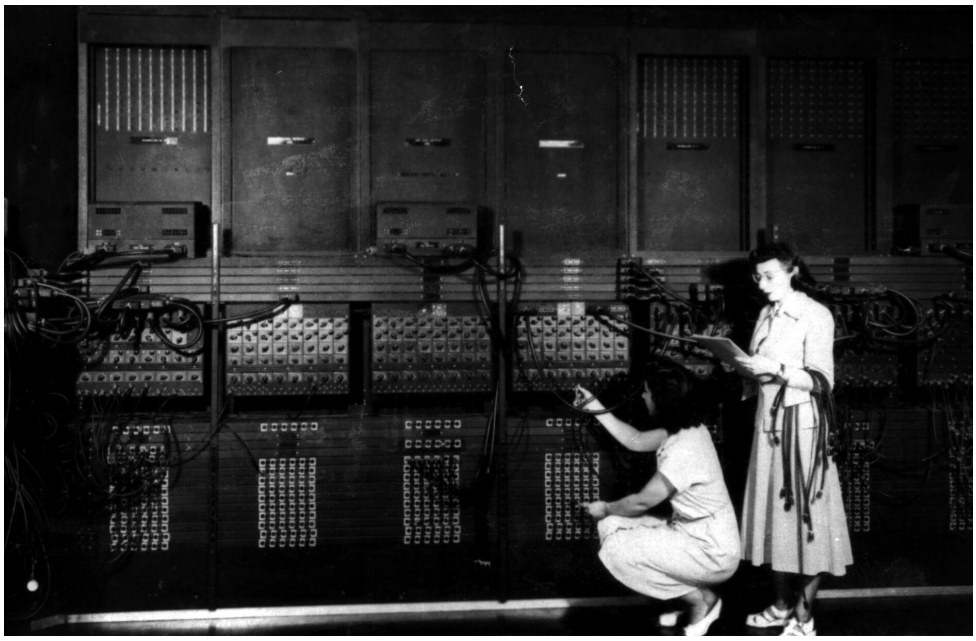

Figure 2: Programmers Ruth Lichterman and Marlyn Wescoff working on the ENIAC computer. U.S. Army photo [10].

Nowadays, global NWP forecasts are routinely made by many weather services using some of the largest supercomputers in the world. Predictions of atmospheric parameters such as temperature, wind, and rain are usually disseminated as a grid of data points on an equirectangular map projection. Figure 3 shows a global NWP temperature forecast on an equirectangular map. These data are used in the examples presented throughout this article. The data in Figure 3 are on a $2.5° \times 2.5°$ rectangular grid for clarity. However, data are routinely available at much higher spatial resolution. For example, the Australian Bureau of Meteorology runs a global NWP model with a latitudinal grid point separation of $0.117\,788°$ and longitudinal spacing of $0.175\,78°$ [6].

The equirectangular map projection is simple and easy for users to process. However, it has some deficiencies. For example, although about $26\,\%$ of the grid points in Figure 3 lie polewards of the polar circles, the polar regions only cover about $8\,\%$ of the

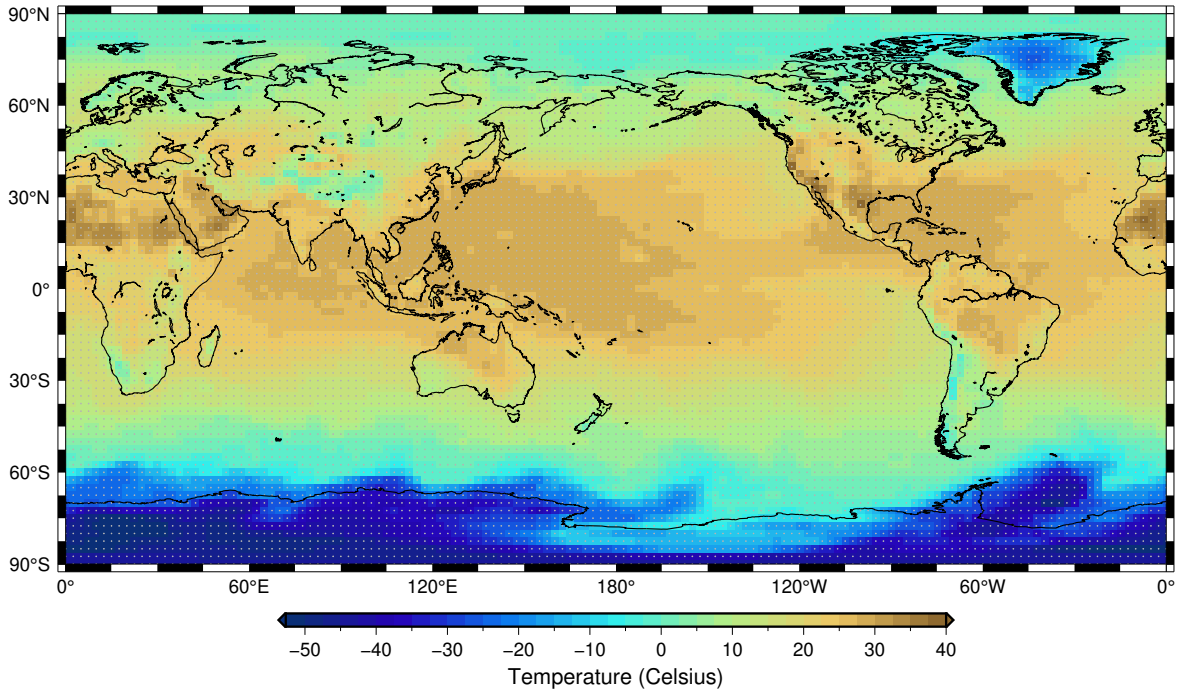

Figure 3: A forecast of temperature $2\,\mathrm{m}$ above the ground from the U.S. National Centers for Environmental Prediction Global Forecast System model. The forecast is valid at 00:00Z on 2 September 2020.

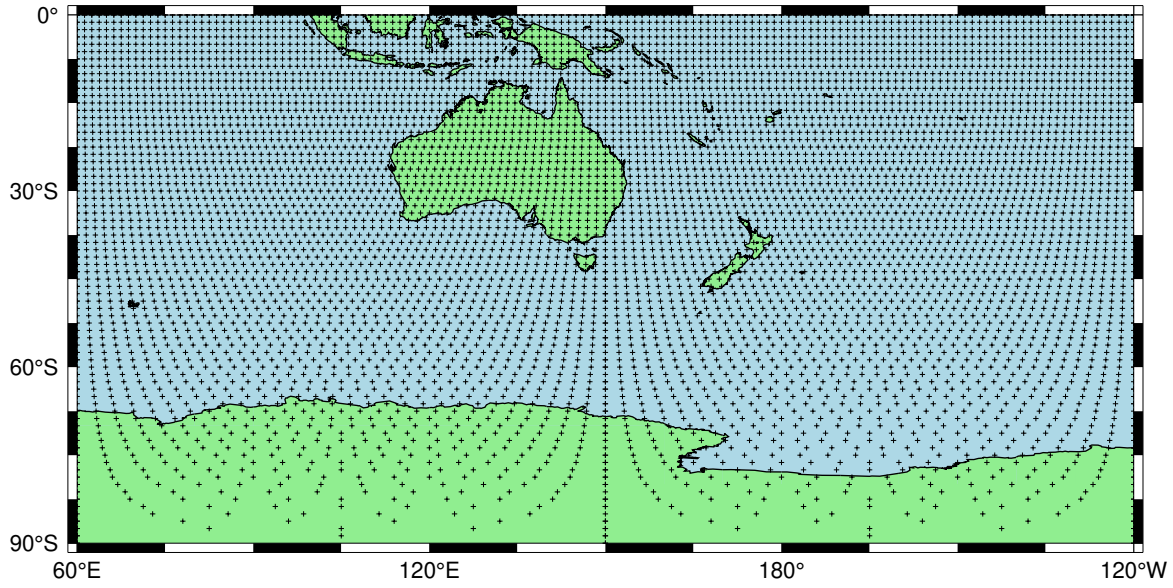

Figure 4: Example of a thinned grid used to disseminate NWP data for two octants of the globe in the Australian region. The spacing of the grid points is $1.25°$ at the equator, and increases on parallels closer to the poles.

Earth's surface[2]. Computation of the area of the polar regions on a spherical Earth is an interesting maths problem left to the reader.

NWP data for aviation use are produced by the World Area Forecast Centres in the United Kingdom and the United States. Historically, data were disseminated on a "thinned" grid, to deal with the multitude of grid points near the poles. In a thinned grid, the number of points on parallels (circles of constant latitude) decrease towards the poles, as illustrated in Figure 4. Thinned grids reduce the size of the data files sent to users. However, in recent years they have fallen out of use as data formats have changed, and communication networks have become faster and cheaper.

This article revisits the concept of thinned grids, using the Euler spiral map projection. In addition to reducing the number of grid points disseminated to users, this projection has some other useful properties when used with meteorological data.

A brief introduction to cartography

Cartography is the study of maps. Maps have been discovered dating back to Babylonian times, if not earlier [11]. As early as the sixth century BC Thales of Miletus developed the Gnomonic projection for star maps [8]. It would have become apparent to early cartographers that mapping a sphere to a flat surface always introduces distortion. However, it wasn't until 1827 that Gauss proved that every projection from a

[2]The polar circles are currently located at $66°33'48.2''$ north and south of the Equator.

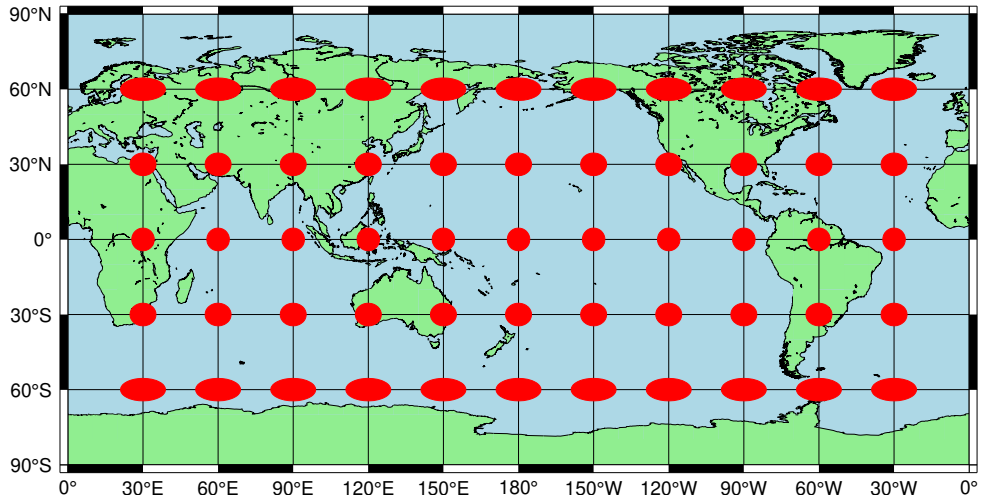

Figure 5: Tissot's indicatrices on the equirectangular map projection.

spherical to a flat surface must create some distortion [5].

A useful graphical tool to display the distortion in a map projection is the Tissot's indicatrix [9]. To construct these indicatrices, we project circles with infinitesimal radius from the surface of the Earth to the map. The projection of a circle to the map will be elliptical. We then rescale the ellipses to a convenient size for viewing. A mathematical treatment of the indicatrices can be found in [8]. Figure 5 shows indicatrices on the equirectangular map projection. The distortion in the map is readily apparent. Small areas appear much larger in the map projection in the polar regions than at low latitudes.

For the dissemination of numerical weather prediction data, it would be useful if the area of each grid cell is equal, no matter where on the Earth that cell is. An equal-area map projection is required to achieve this. The sinusoidal map projection (Figure 6) is an example of one of the first equal-area map projections, developed during the Sixteenth Century [2]. Examining the Tissot's indicatrices in Figure 6, it is apparent they are the same area at all locations. However, the shape distortion increases away from the Equator and central meridian.

The Euler spiral map projection

It would be nice to have a map projection which is not only equal-area but also does not distort the shape. At first, this might seem unlikely, given a sphere cannot be flattened onto a plane without distortion. A 2012 paper by Bartholdi and Henriques studied the shape a spiral orange peel would take when flattened onto a plane, as shown in Figure 7 [1]. As the width of the peel becomes thinner, they showed the distortion in the flattened peel becomes smaller, and the shape of the flattened peel tends towards an Euler spiral. However, the flattened peel would need to be infinitesimally thin to be distortion-free.

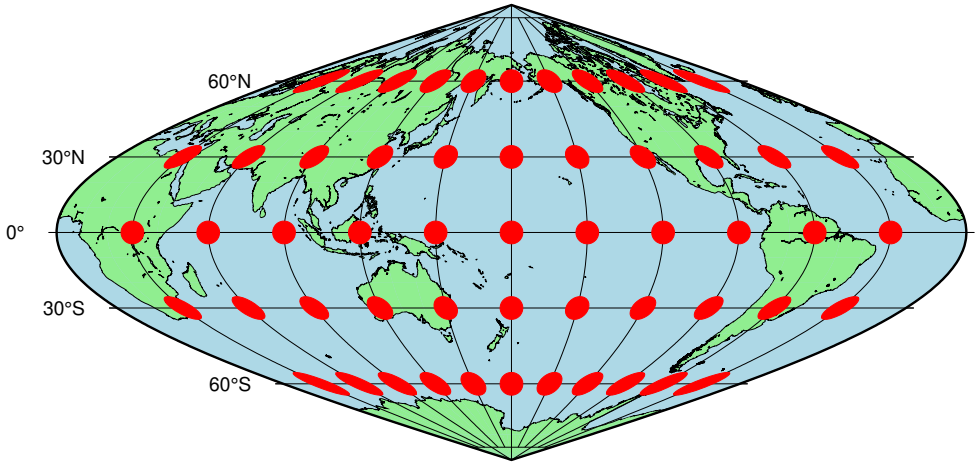

Figure 6: Tissot's indicatrices on a sinusoidal projection of the Earth.

If the orange peel is width $\frac{1}{N}$ on a sphere of unit radius, then Bartholdi and Henriques showed that the flattened peel is parameterised by the equations

$$\begin{cases} x(t) &= \int_0^t \cos\sqrt{(2\pi N)^2 - u^2}du, \\ y(t) &= -\int_0^t \sin\sqrt{(2\pi N)^2 - u^2}du. \end{cases} \tag{1}$$

Here, t ranges from $-2\pi N$ at the south pole to $2\pi N$ at the North Pole of the sphere.

If instead of an orange, one imagines peeling the surface of the Earth, it is evident we have a new type of map projection. Figure 1 shows the Euler spiral map projection.

2 Applying the Euler spiral projection to meteorological data

The NWP data shown in Figure 3 are on a $2.5°\times2.5°$ equirectangular map grid. The grid box spacing in radians, $\Delta\phi$, is

$$\Delta\phi = 2.5 \times \frac{2\pi}{360} \approx 0.0436\,\text{rad}. \tag{2}$$

The distance between adjacent grid points on a meridian is thus

$$d = R_e\Delta\phi \approx 278\,\text{km}, \tag{3}$$

where R_e is the radius of the Earth and d is the distance between grid points on a meridian. The Earth is assumed to be spherical, with a radius of approximately $6371\,\text{km}$. In reality, the Earth is an oblate spheroid, but the difference from a sphere is minor[3]. As

[3]The polar radius of the Earth is $6356.8\,\text{km}$, the equatorial radius is $6378.1\,\text{km}$ and the mean radius is $6371.0\,\text{km}$.

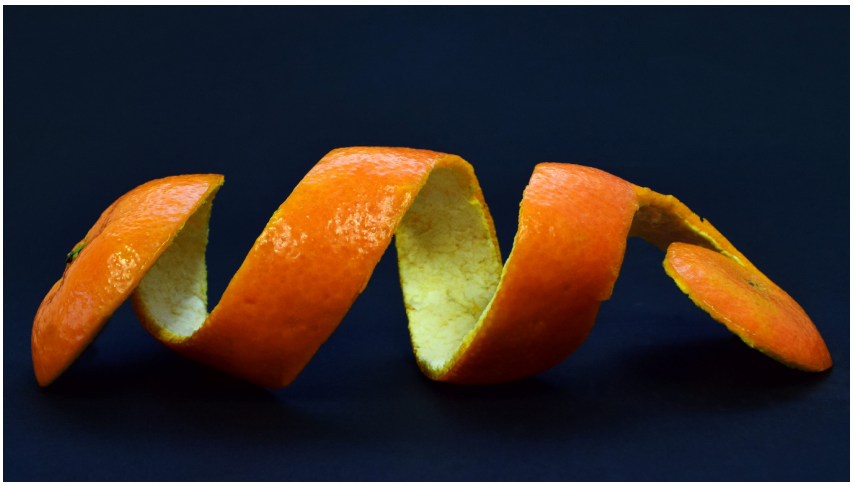

Figure 7: Peeling an orange in a spiral. Public domain image obtained from https://www.pikrepo.com/feawc/orange-spiral-skin-artwork.

discussed earlier, the distance between adjacent grid points on the parallels decreases as the poles are approached. This results in an increased density of grid points in the polar regions.

A small grid box on the equator of the equirectangular map covers an area, A, of approximately

$$A \approx R_e^2 \Delta\phi^2 \approx 77\,277\,\mathrm{km}^2. \tag{4}$$

Equation 4 is not exact, because the small grid box forms a portion of a spherical surface, not a plane. However, the approximation becomes more accurate as the grid box decreases in size. If the Earth were to be tiled in grid boxes with this area, the number of grid boxes, n, to cover the whole surface would be

$$n = \frac{4\pi R_e^2}{R_e^2 \Delta\phi^2} = \frac{4\pi}{\Delta\phi^2} \approx 6600. \tag{5}$$

However, the equirectangular map grid in Figure 3 contains $144 \times 73 = 10512$ grid points. Remapping the NWP data to an equal-area map projection reduces the number of grid cells required to cover the Earth by $37\,\%$. This reduction leads to smaller file sizes and faster transmission times when sending the data to users. However, it comes at the expense of coarser spatial resolution in the polar regions.

Figure 8 illustrates the process of mapping NWP data to the Euler spiral map projection. Points are laid out on a spiral starting at the South Pole, and terminating at the North Pole. The spiral width is the same as the spacing of adjacent grid points along a meridian in the original equirectangular map projection. For the $2.5° \times 2.5°$ data presented earlier, this is approximately $278\,\mathrm{km}$. The distance between adjacent points on the spiral is the same as the distance between adjacent points on the equator of the equirectangular map. For the example data, this is also $278\,\mathrm{km}$. Consequently, every point on the spiral represents an almost equal-area square region of $278\,\mathrm{km} \times 278\,\mathrm{km}$.

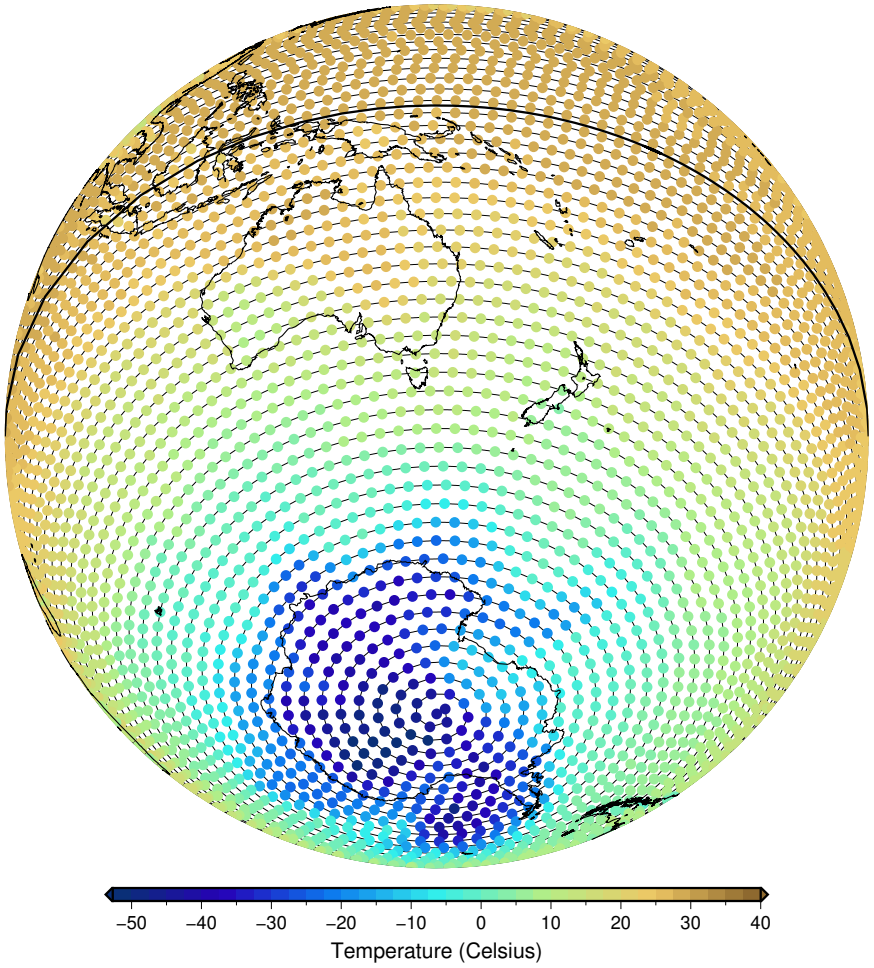

Figure 8: Orthographic map of the Earth illustrating how points can be laid out in a spiral on the globe so they have equal area. When this spiral is flattened out, it forms the Euler spiral map projection shown in Figure 9.

We interpolate data from the original equirectangular projection in Figure 3 to the spherical spiral using bilinear interpolation.

Figure 9 shows the spiral in Figure 8 flattened to an Euler spiral on a plane. It appears that much of the spatial information in the original temperature field is lost. However, "re-wrapping" the Euler spiral around the globe recovers this information. This task is conceptually no more complicated than processing data on the thinned grid shown in Figure 4.

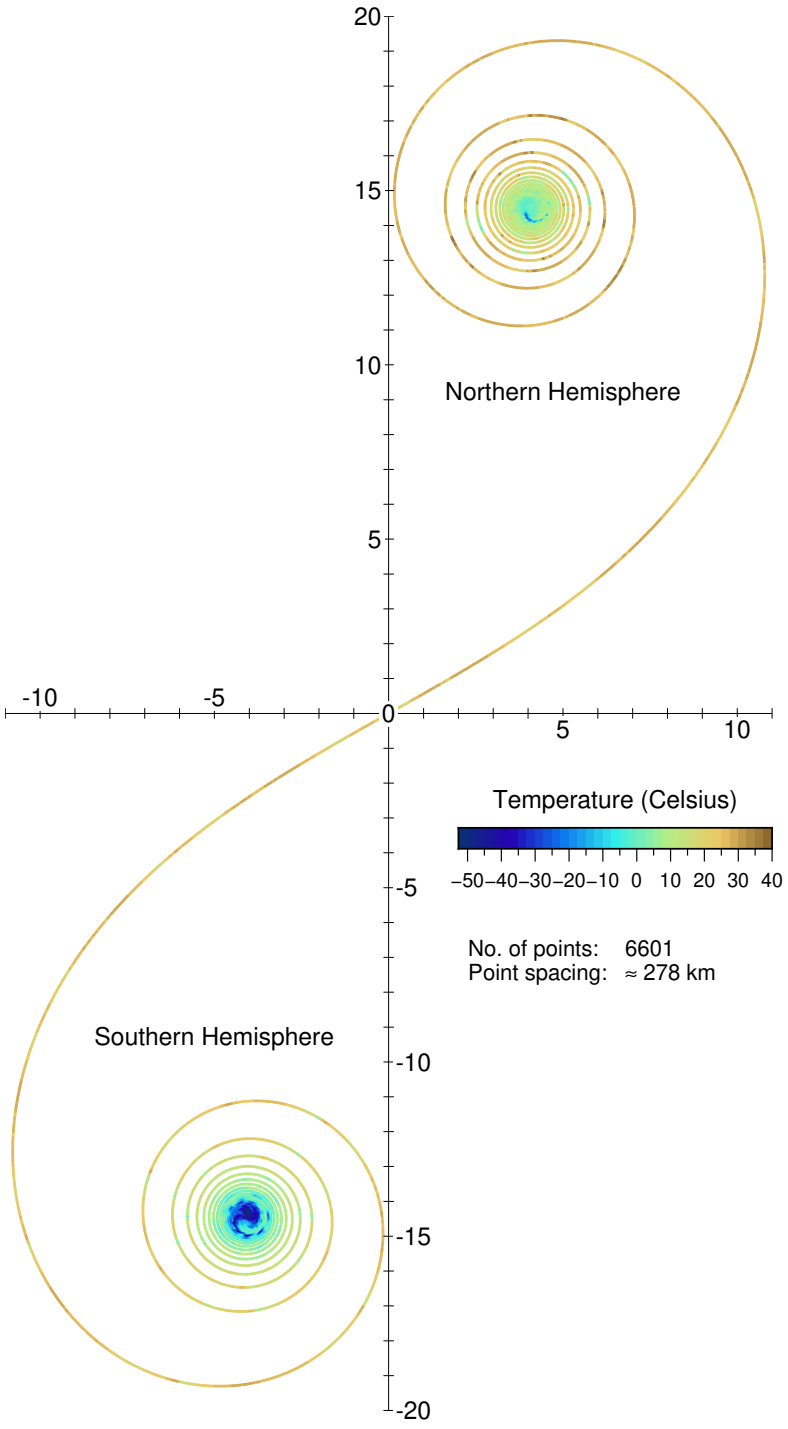

Figure 9: The temperature data mapped onto the Euler spiral map projection. Distances are in units of Earth radii, R_e.

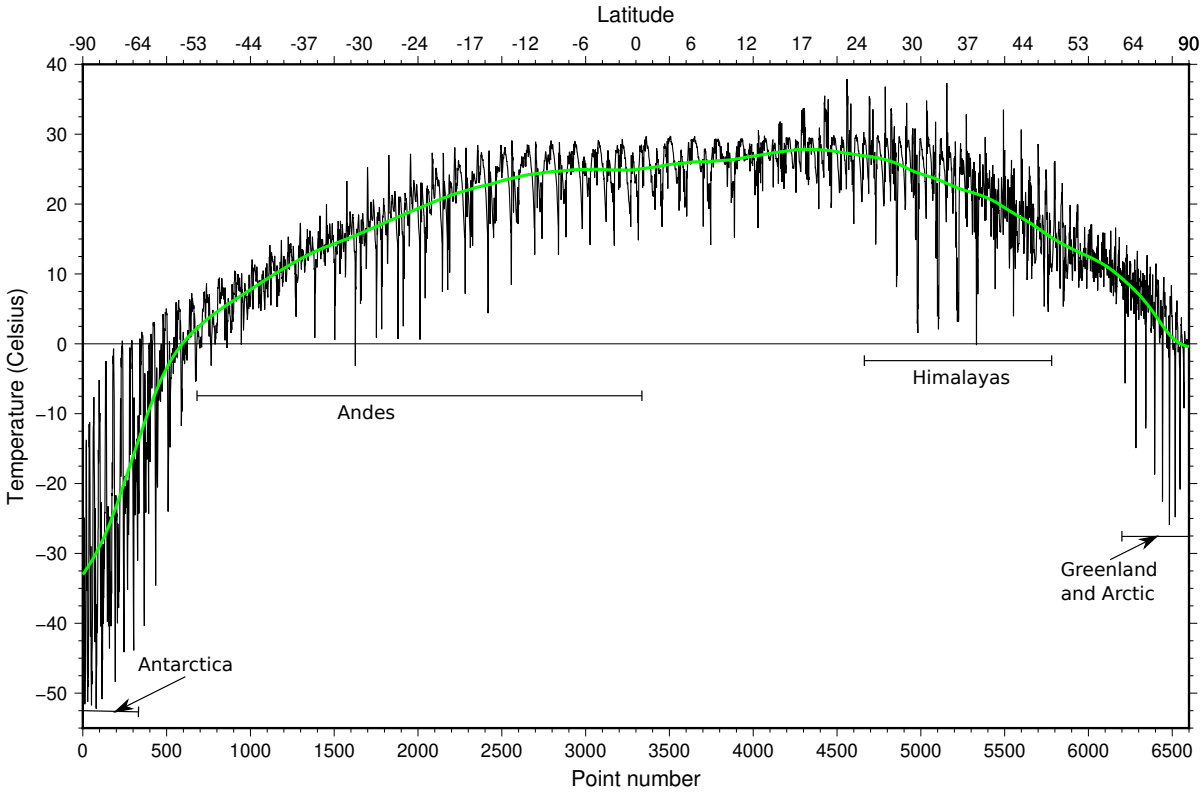

Figure 10: Temperature displayed as a function of distance from the South Pole end of the Euler spiral map projection.

3 Some useful properties of the Euler spiral map projection

The Euler spiral projection displayed in Figure 9 also provides a new way to reference any NWP data point on the globe. We can reference data points by their distance from the beginning of the spiral, instead of a latitude and longitude. The projection has taken a two-dimensional data array and flattened it onto a single dimension. Figure 10 shows the data plotted as a function of the point's distance from the beginning of the spiral.

The black line in Figure 10 shows the temperature starting at the South Pole and ending at the North Pole. The latitudes of points in the spiral form an increasing series, shown on the top axis of the diagram. The thick green line is created by passing a Gaussian filter with a width of 432 points over the data. The Gaussian filter removes the high-frequency variations in the temperature data to highlight the relationship between temperature and latitude.

Displaying the data this way highlights several features. Firstly, the highest frequency variations in temperature occur because the spiral alternately travels through

the day and night sides of the Earth; the night-time side is usually colder than the day-time side. The oceans never fall below $0\,^{\circ}\mathrm{C}$. Temperatures higher than $0\,^{\circ}\mathrm{C}$ are seen at latitudes north of about 68°S because the spiral traverses at least some ocean at these latitudes. Polewards of 68°S, points are either over sea ice or Antarctica. Lower temperatures occur over high mountain ranges. The effect of the Andes and Himalayas are readily apparent in the regions indicated in the diagram. The Greenland ice sheet is also evident because it is colder than its surrounds.

Another property of equal area map projections is that they make the computation of global averages easy. Because each grid cell has equal-area, the global average is simply

$$\bar{T} = \frac{1}{n} \sum_{i=0}^{n} T_i \tag{6}$$

where n is the number of points on the spiral, T_i is the value of the variable being averaged at each point on the spiral, and $\bar{T}$ is the global average of the variable. To compute the global average of data on the standard equirectangular grid would require differing weights for each grid cell based on their area. The global average temperature of the data shown in the preceding figures is $15.8\,^{\circ}\mathrm{C}$.

4 Conclusions and further reading

The Euler spiral map projection can significantly reduce the number of NWP grid points required to cover the globe, compared to the usual equirectangular map. We showed that the number of points in the Euler spiral grid was $37\,\%$ less than the rectangular grid.

Although the author does not anticipate the widespread use of this technique to compress NWP data, there may be specialised applications where the compression and other properties of the Euler spiral map projection are useful. Meteorological data compression remains an important topic. With the increase in computer power, the volume of meteorological data generated daily has exploded. Some weather forecasting agencies maintain magnetic tape archives hundreds of petabytes in size. Writing and retrieving data to and from magnetic tape is slow, so savings gained from data compression are vital.

Hopefully, readers have found this introduction to meteorology, cartography and the Euler spiral map projection interesting. All references in the article are available on the web; hyper-links are provided in the bibliography. Some other suggestions for further reading and investigation are listed below.

Map Projections – A Working Manual is a valuable and practical introduction to cartography [8]. For a fascinating new class of map projections known as myriahedral projections, see Wijk [12]. The open-source Generic Mapping Tools (GMT) created all the maps presented in this article. GMT is available from `https://www.generic-mapping-tools.org/` [13].

Real-time NWP data are available from the U.S. National Centers for Environmental Prediction (NCEP: `https://nomads.ncep.noaa.gov/`). A NASA software package,

Panoply, can easily display data obtained from the NCEP site on a range of map projections. Panoply is available from https://www.giss.nasa.gov/tools/panoply/.

References

[1] L. Bartholdi and A. Henriques, Orange peels and Fresnel integrals, *The Mathematical Intelligencer* **34** (2012), 1–3. https://link.springer.com/content/pdf/10.1007/s00283-012-9304-1.pdf, last accessed 2021-04-24.

[2] J. Cossin, Carte cosmographique et universelle description du monde avec le vrai traict des vents, *Bibliothèque nationale de France*, 1570. https://gallica.bnf.fr/ark:/12148/btv1b5901087w/f1.item, last accessed 2021-04-24.

[3] J.G. Charney, R. Fjöftoft and J. von Neumann, Numerical integration of the barotropic vorticity equation, *Tellus* **2** (1950), 237–254. https://www.tandfonline.com/doi/pdf/10.3402/tellusa.v2i4.8607, last accessed 2021-04-24.

[4] H. Fry, A strange map projection, *Numberphile*, B. Haran (ed.), https://www.numberphile.com/videos/strange-map-projection, last accessed 2021-04-24.

[5] K.F. Gauss, *General Investigations of Curved Surfaces of 1827 and 1825*, translated by J.C. Morehead and A.M. Hiltebeitel, The Princeton University Library, 1902. http://www.gutenberg.org/files/36856/36856-pdf.pdf, last accessed 2021-04-24.

[6] National Operations Centre, *NOC Operations Bulletin Number 125, APS3 upgrade of the ACCESS-G/GE Numerical Weather Prediction system*, Australian Bureau of Meteorology, 2019. http://www.bom.gov.au/australia/charts/bulletins/opsbull_G3GE3_external_v3.pdf, last accessed 2021-04-24.

[7] L.F. Richardson, *Weather Prediction by Numerical Process*, Cambridge at the University Press, 1922. https://archive.org/details/weatherpredictio00richrich/, last accessed 2021-04-24.

[8] J.P. Snyder, *Map projections – a working manual* Professional paper; 1395, U.S. Geological Survey, 1987. https://pubs.usgs.gov/pp/1395/report.pdf, last accessed 2021-04-24.

[9] A. Tissot, *Mémoire sur la Représentation des Surfaces*, Imprimerie de Gauthier-Villars, Paris, 1881.
https://archive.org/details/mmoiresurlarepr00tissgoog,
last accessed 2021-04-24.

[10] U.S. Army, Historic Computer Images, M. Muus (ed.), ARL *Technical Library*.
https://ftp.arl.army.mil/ftp/historic-computers/png/eniac4.png,
last accessed 2021-04-24.

[11] The British Museum, *Object: The Map of the World*.
https://www.britishmuseum.org/collection/object/W_1882-0714-509,
last accessed 2021-04-24.

[12] J.J. van Wijk, Unfolding the Earth: myriahedral projections, *The Cartographic Journal* **45** (2008), 32–42.
https://www.win.tue.nl/~vanwijk/myriahedral/CAJ103.pdf,
last accessed 2021-04-24.

[13] P. Wessel, J.F. Luis, L. Uieda, R. Scharroo, F. Wobbe, W.H.F. Smith and D. Tian, The Generic Mapping Tools version 6, *Geochemistry, Geophysics, Geosystems* **20** (2019), 5556–5564.
https://agupubs.onlinelibrary.wiley.com/doi/epdf/10.1029/2019GC008515, last accessed 2021-04-24.